RESEARCH ARTICLE

L-Lactic acid biosensor based on multi-layered graphene

Antonio Radoi · Alexandru Cosmin Obreja ·
Sandra A. V. Eremia · Adina Bragaru ·
Adrian Dinescu · Gabriel-Lucian Radu

Abstract Pristine graphene platelets and graphene oxide were used as electrode modifiers, aiming the investigation of their electrochemical efficacy towards β-nicotinamide adenine dinucleotide (NADH). The electrochemical detection of NADH is one of the most studied areas of bioelectro-analysis because of the ubiquity of NAD(P)H-based enzymatic reactions in nature. Commercially available graphene and laboratory prepared graphene oxide were used to modify glassy carbon electrodes and the behaviour of such modified electrodes against potassium ferricyanide (III) and NADH was reported. Relying on the graphene-modified transducer, L-lactic dehydrogenase (L-LDH) was successfully immobilised in a 1 % Nafion® membrane. The developed biosensor, working at +250 mV versus Ag/AgCl reference electrode, was used to assess L-lactic acid in four different types of yogurts, revealing an L-lactic acid concentration ranging between 0.3 and 0.6 %.

Abbreviations
NADH	β-nicotinamide adenine dinucleotide
NAD^+	Oxidised form of β-nicotinamide adenine dinucleotide
G	Graphene
GO	Graphene oxide
GC	Modified glassy carbon
L-LDH	L-lactate dehydrogenase

A. Radoi (✉) · A. C. Obreja · A. Bragaru · A. Dinescu
National Institute for Research and Development in
Microtechnology (IMT-Bucharest), 126A Erou Iancu Nicolae,
077190 Bucharest, Romania
e-mail: radoiantonio@yahoo.com

S. A. V. Eremia · G.-L. Radu
Centre of Bioanalysis, National Institute of Research and
Development for Biological Sciences, 296 Splaiul
Independentei, 060031 Bucharest, Romania

1 Introduction

Carbonaceous-based materials are extensively used in many research fields, potential applications spanning from electric double-layer capacitors [1], energy production [2], field emission [3] or electrochemistry [4]. Carbon is a versatile element, and can be present as various allotropes including graphite, diamond and fullerene-like structures. Belonging to the carbon family, carbon nanotubes [5] (CNTs) consist of seamlessly rolled up graphene layer(s), meanwhile only graphene differentiates as a two-dimensional material, made of a single monolayer of carbon atoms [6]. Graphene is considered to be important in the electrochemistry field [7], since it has high electron conductivity [8], fast heterogeneous electron-transfer rate [9], high surface area [10] and also it can be obtained at affordable costs [11].

The relevance of β-nicotinamide adenine dinucleotide (NADH) as cofactor in naturally occurring enzymatic reactions, as well as the potential applications in developing NADH-based biosensors are still considered as key aspects in the bio-electro-analytical research field [12–18]. The electrochemistry of the redox couple NAD^+/NADH has been intensively studied by Gorton [19]; and the formal redox potential (E°′) of the NAD^+/NADH is known to be −560 mV versus SCE [20]. Even if it is still controversial, however, a sequential electrochemical-chemical-electrochemical mechanism is widely accepted to be the path undertaken in NADH oxidation. Direct electrochemical

oxidation of NADH to its corresponding oxidised form (NAD^+) at the bare/unmodified electrodes is highly irreversible, requires large activation energy, and proceeds with coupled side reactions, poisoning the electrode [21, 22]. The decrease of the anodic oxidation overpotential may be achieved using redox mediators [23–25], carbon in various hybridizations and forms [26–28], boron-doped diamond [29], metallic sputtered CNTs [30], single crystal gold [31] or carbon paste electrode modified with nickel oxide nanoparticles [32]. The advancement of graphene-based biosensors has been reviewed [33, 34] and the NADH-based biosensors relaying on the use of graphene or graphene derived materials (such as GO or reduced GO) were reported by several worldwide research groups [35–38].

In this paper, we report the preparation and analytical characterisation of multi-layered graphene and graphene oxide (GO)-modified glassy carbon (GC) electrode used for NADH. This electrochemical sensing probe was further utilised as transducer for the development of an L-lactate biosensor. This L-lactate biosensor, working at an applied potential of +250 mV versus Ag/AgCl reference electrode, was used to determine L-lactic acid in several types of yogurts, illustrating that the concentration of L-lactic acid was correlated with the percentage of fat in the analysed samples.

2 Experimental

2.1 Materials, reagents and instrumentation

Graphene was supplied by NanoIntegris, USA (PureSheets[TM] QUATTRO) as a water-based dispersion (0.05 mg/mL) containing 2 % (w/v) ionic surfactant. Graphite flakes (SP1) were from Bay Carbon, Inc., USA. Spectral graphite rods ($d = 2$ mm) were provided by Elektrokarbon a.s. (Slovak Republic).

NADH (purity ≥97 %) was purchased from Santa Cruz Biotechnology, Inc. (http://www.scbt.com/). L-lactate dehydrogenase (∼140 IU/mg), NAD^+ (>95 %, HPLC), L-lactic acid, Nafion® 5 % (v/v) solution, $NaNO_3$, H_2SO_4, $KMnO_4$, HCl, H_2O_2, hydrazine monohydrate, isopropanol, diethyl ether potassium phosphate dibasic, potassium dihydrogen phosphate, potassium chloride, potassium permanganate and all the other reagents used for buffers were from Sigma–Aldrich. PTFE-membrane filters (0.5 μm pore size) from Carl Roth GmbH (http://www.carlroth.com) were also used. All chemicals from commercial sources were of analytical grade. A colorimetric assay kit (R-Biopharm AG, Darmstadt, Germany) for L-lactic acid was also used.

Glassy carbon electrodes, $d = 3.0$ mm, were supplied by Bioanalytical Systems (BAS, West Lafayette, USA). PK-3 electrode polishing kit (0.05 μm alumina and 1 μm diamond) was purchased from Bio-Logic SAS (http://www.bio-logic.

info). Electrochemical investigations were performed using the Autolab electrochemical system (Eco Chemie, The Netherlands). All electrochemical measurements were performed with a three electrode configuration. Potentials were measured versus the Ag/AgCl reference electrode obtained from BAS West Lafayette, USA. A platinum wire was used as the auxiliary electrode. Nova NanoSEM 630 (FEI Company, USA) was used for scanning electron microscopy (SEM) investigations and Allegra X-22 (Beckman Coulter) centrifuge was used for yogurt sample pre-treatment. Yogurt samples were from local suppliers.

2.2 Graphene oxide synthesis and graphene preparatory

Graphene oxide was prepared accordingly to Hummers method [39], slightly modified [40]. Basically 2 g of graphite flakes and 1 g of $NaNO_3$ were mixed with 46 mL of concentrated H_2SO_4, under continuous stirring and controlled temperature (5 °C). $KMnO_4$ (6 g) was added and the temperature was maintained below 5 °C for at least 60 min; the reaction was allowed to proceed by carefully monitoring the temperature in order not to exceed 35 °C. The reaction slurry was gradually diluted using 300 mL of deionized water and the unreacted $KMnO_4$ was neutralized by adding 5 % v/v solution of H_2O_2 (50 mL). The reaction mixture was filtered on a sintered glass filter (medium pore size); sulphate salts were removed by using HCl solution (5 % v/v) and plenty of deionized water. The obtained cake was dried under vacuum, at 80 °C, during 48 h. A stable dispersion of GO (1 mg/mL) was achieved after ultrasonication, for about 30 min in water, and further used to modify the electrodes as described in Sect. 2.3.

Surfactants are necessary to avoid agglomeration and precipitation of graphene platelets [41], but removal of surfactant is a key aspect for graphene to preserve its intrinsic properties. The commercial available graphene consisted of: 27 % single layer, 48 % double layer, 20 % triple layer and 5 % four or more layers and does not have any graphite impurities. A detailed technical specification sheet, including also atomic force microscopy characteristics is available at: www.nanointegris.com. Since graphene was supplied as water-based dispersion containing 2 % (w/v) ionic surfactant, we proceed with the removal of the surfactant. For such a reason a certain volume of the received graphene dispersion was mixed with isopropanol and diethyl ether (1:1:2 v/v/v), by using a glass rod. Allowing few minutes to settle down, graphene platelets gathered in a fine layer, at the interface between the organic (i.e. diethyl ether) and the aqueous phase (i.e. mixture of isopropanol and water), by selective partition and floated at the interface due to the large surface available (2,630 m^2/g) [10]. The graphene suspension was removed and dispersed

again by ultrasounds in 50 mL of distilled water; again the above described process was repeated five times, and in the end, the purified graphene platelets were dried under vacuum, at 80 °C, during 48 h. A stable dispersion of graphene (1 mg/mL) was achieved in water:ethanol (1:1 v/v), with ultrasonication for 30 min, and further used to modify the electrodes as described in Sect. 2.3.

2.3 Preparation of modified electrodes

Several types of electrodes were prepared for our electrochemical studies. Prior modification, GC electrodes ($d = 3.0$ mm) were mechanically polished (PK-3 Electrode Polishing kit), immersed in distilled water in an ultrasonic bath (20 s.) and electrochemically cleaned, in 0.1 M H_2SO_4 solution using cyclic voltammetry, by performing 35 scans, at 50 mV/s, sweeping between -300 mV and $+1,200$ mV. Glassy carbon electrodes were modified by using 4 µL from the respective graphene or GO dispersions and allowed to dry under a moderate stream of nitrogen. Lactate biosensors were prepared by adsorbing L-lactate dehydrogenase on graphene-modified electrode and thereafter 5 µL of 1 % (v/v) Nafion® neutralized solution were casted and allowed to dry. The L-lactate biosensor, when not used, was stored in 10 mM phosphate buffer saline (PBS), at 4 °C. After investigating the effect of enzyme loading, 20 IU of L-lactic dehydrogenase (L-LDH)/electrode were selected to be the best enzyme loading among 5, 10, 20 and 40 IU of L-LDH. The concentration of the cofactor (NAD^+) was also optimised. It was found that 3 mM NAD^+ was the best concentration, (from 0.5, 3.0 and 6.0 mM investigated concentrations of cofactor), to be used for the analytical determination of L-lactic acid, with the proposed biosensor. The optimised pH value was found to be 7.5. The biosensor working applied potential was $+250$ mV versus Ag/AgCl reference electrode.

2.4 Sample preparation

Commercially available yogurt samples were bought from local markets. Samples were centrifuged during 15 min at 6,000 rpm, and the supernatant was carefully collected, filtered through 0.5 µm PTFE-membrane filters and diluted, prior analysis, in 10 mM PBS.

3 Results and discussion

3.1 Characterisation of graphene oxide and graphene

Scanning electron microscopy (SEM) investigations revealed that there was a significant difference in the morphology of graphene and GO. SEM micrographs illustrated
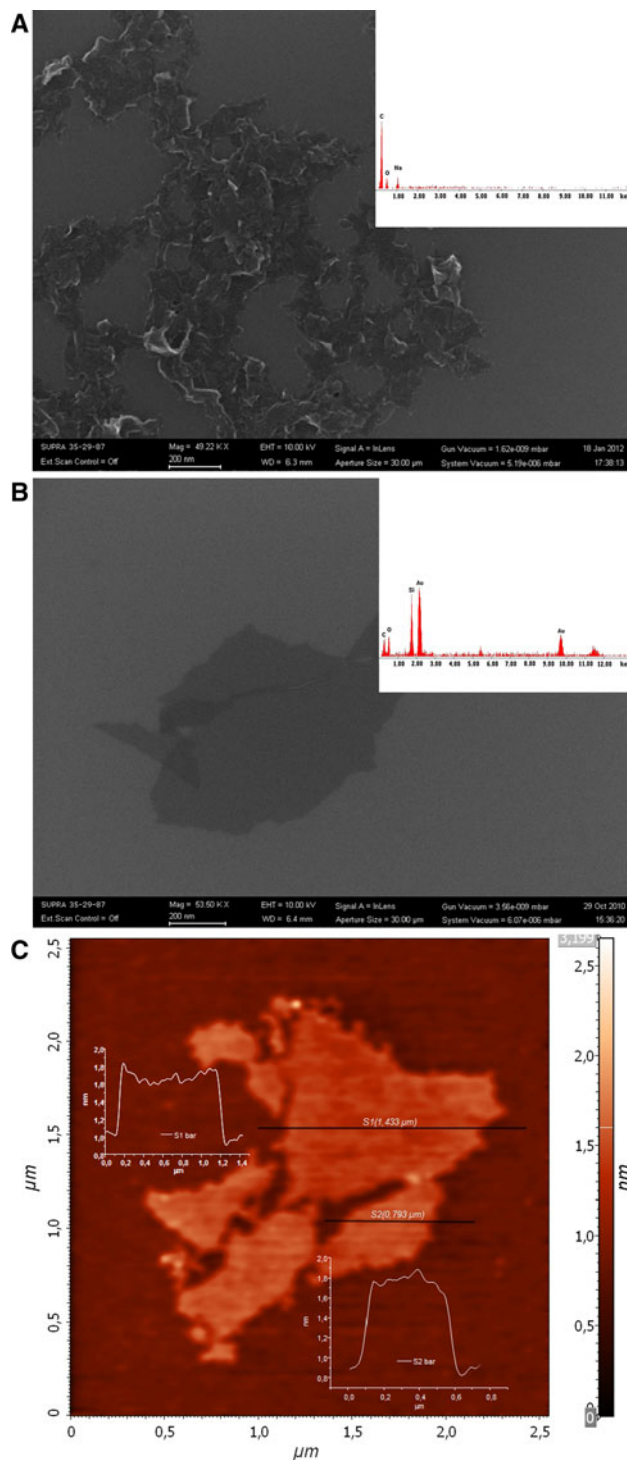
Fig. 1 Microscopic images illustrating: **a** wrinkled graphene with uneven edges after surfactant removal (*inset* the energy dispersive X-ray spectrum is depicted), **b** flat graphene oxide with sharp edges (*inset* the energy dispersive X-ray spectrum is also depicted; Si and Au peaks are ascribed to the support substrate), **c** graphene oxide atomic force microscopy with height profiles

in Fig. 1a, b depicted wrinkled graphene sheets with uneven and swollen margins, while home-made GO was flat with even edges. Energy dispersive X-ray spectra indicated that
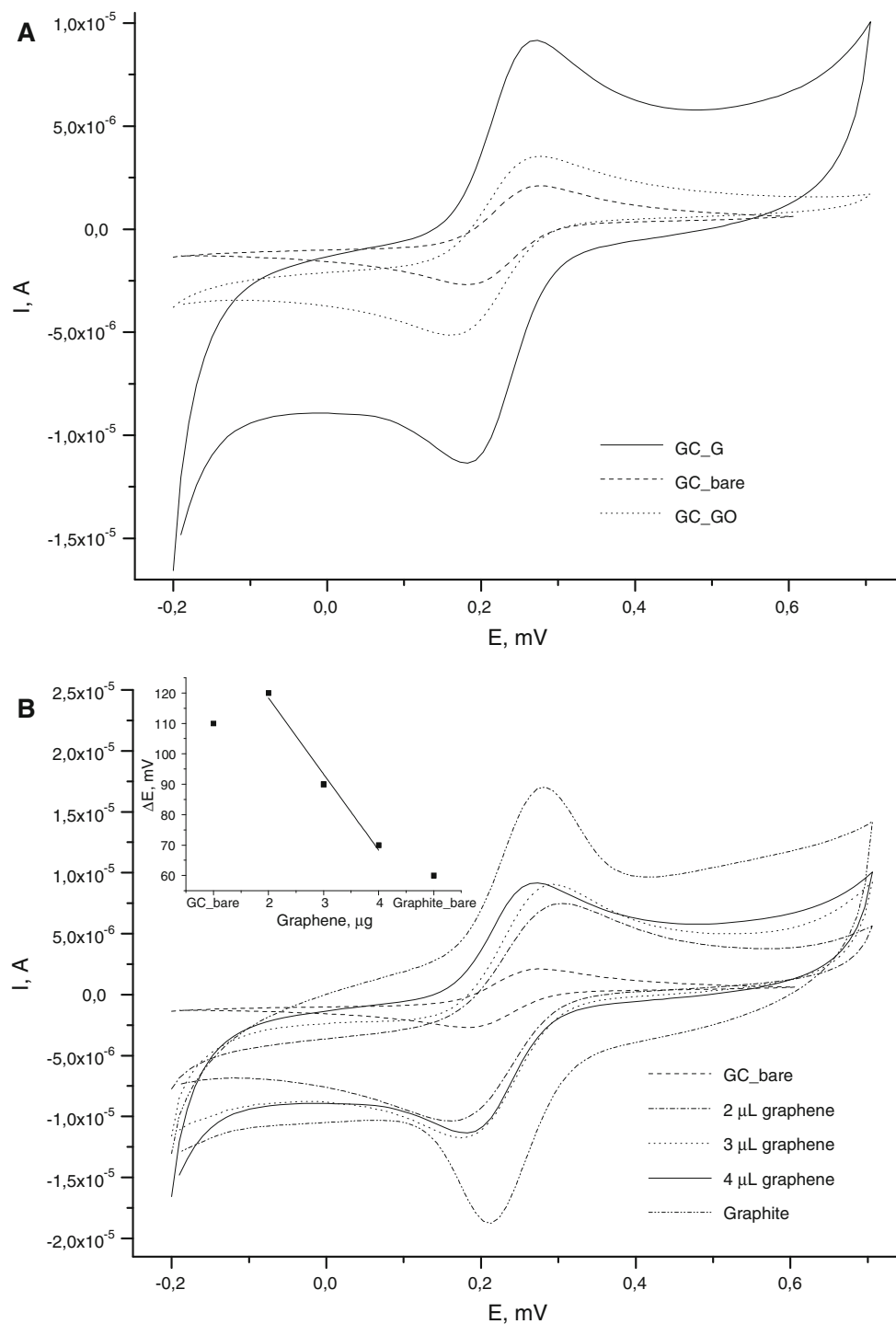
Fig. 2 Cyclic voltammetry recordings illustrating: **a** the behaviour of bare glassy carbon electrode (GC_bare), graphene (GC_G) and graphene oxide (GC_GO)-modified electrodes, **b** the electrode coverage study and relationship between the mass of graphene deposited upon the electrode surface and the resultant peak separation (*inset*) and **c** the behaviour of GC_G electrode at different scan rates illustrating that the response of the electrode is purely diffusional (*inset* C1 and C2)

the ratio of C to O was $\sim$6:1 in graphene, meanwhile for GO this ratio was roughly 1:1, due to the presence of oxygen functionalities (i.e. hydroxyl, epoxy, carboxyl groups, etc.) on the surface of graphene sheets, and also indicated that the

oxidation process has been achieved. Graphene supplied by NanoIntegris is supposed to be entirely pristine graphene platelets that have not been oxidised, reduced or chemically modified in anyway, and we assumed that the presence of

Fig. 2 continued
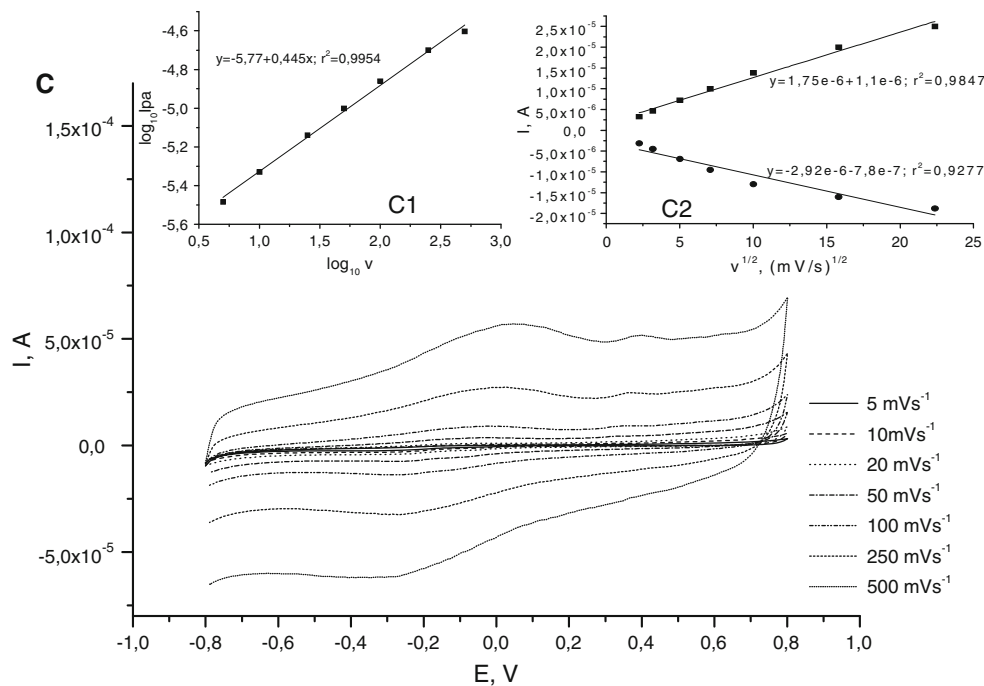
oxygen in EDX spectrum is due to adsorbed oxygen. Moreover, the presence of sodium indicated that traces of surfactant were still present, even after five washing steps.

Atomic force microscopy (Fig. 1c) performed on GO illustrated that the flake thickness ($\sim 0.8 - 0.9$ nm) was typical for single-layered GO [42].

3.2 Electrochemical characterisation of the modified electrodes

In order to rationalise on the electrocatalytic behaviour of the modified GC electrodes, as a preliminary assay, we used potassium ferricyanide (1 mM) in supporting electrolyte to investigate peak separation. As it can be seen from Fig. 2a, in the case of the unmodified electrode the peak potential separation ($\Delta E = E_{p_a} - E_{p_c}$) was 110 mV ($E_{p_a} = +283$ mV, $E_{p_c} = +173$ mV), while for the GO-modified GC electrode $\Delta E = 100$ mV ($E_{p_a} = +273$ mV, $E_{p_c} = +173$ mV). Instead graphene-modified GC electrode ($\Delta E = 70$ mV, $E_{p_a} = +263$ mV, $E_{p_c} = +193$ mV) illustrated to be able to drive the electron transfer reaction faster than both bare or GO-modified electrode. The obtained results are in good agreement with the results reported in other studies, illustrating the fast electron transfer behaviour on graphene, for single-electron-based electrochemical reaction [33]. Brownson et al. [43, 44] observed that heterogeneous electron kinetics is influenced by the global coverage of graphene on the electrode surface. Two distinct cases were described: "Zone I"—

corresponding to an incomplete coverage of the underlying electrode surface, predominance of graphene basal planes and reduced electrochemical reactivity, and "Zone II"—made of layered graphene, governance of edge planes and thus increase in heterogeneous electron transfer and improved electrochemical response. By doing this coverage study, we were able to illustrate the case of "Zone II" (Fig. 2b), where increased amounts of graphene casted on the GC electrodes produced a decrease in peak potential separation, approaching the graphite case (Fig. 2b—inset). Peak potential separation for bare graphite rod was 60 mV and for 2, 3 and 4 μL graphene (1 mg/mL graphene stock solution) casted GC electrodes ΔE varied from 120 to 90 mV and finally to 70 mV, respectively. As reported in [43] the ΔE changed with the amount of graphene immobilised on the surface of the underlying electrode, reduced peak-to-peak separation illustrating improved electron kinetic ascribed to electrochemically active edge plane sites in "Zone II." In order to discriminate between thin-layer effects and diffusional response at the multi-layered graphene-modified electrode, scan rate was varied in the presence of 1 mM potassium ferricyanide as redox probe. Plots illustrating the logarithm of the anodic peak current versus the logarithm of the scan rate (Fig. 2c) inset c1) gave a slope coefficient of 0.445 close to 0.5. Corroborating this data with the linear correlation obtained from plotting peak current versus the square root of the applied scan rate (Fig. 2c) inset c2), we can assume that the response of the electrode is governed by diffusion.

3.3 Electrochemical behaviour of NADH at the modified electrodes

Considering the performance of an electrochemical sensor, the properties of the electrode material are the most significant. The electrochemical response of graphene sheets (single-, few- and multi-layer graphene) has shown to be independent of the number of layers [7] and does not have tremendous advantages over graphite micro-particles [45]. Nonetheless the combination of its interesting electrochemical properties [43, 44, 46–48] and its peculiar physiochemical properties made graphene beneficial to be utilised in a range of sensing and energy related electrochemical applications. Keeley et al. [48] used exfoliated graphene, obtained in dimethylformamide after prolonged ultrasonication, to investigate the detection of NADH. Under Ar atmosphere, electrochemistry experiments were achieved using a GC electrode modified with graphene nano-sheets. Chronoamperometry, conducted at +0.4 V versus Ag/AgCl, illustrated a LOD in the low micromolar range (1.9 μM) for NADH and a stability improvements over bare GC electrode.

In our experiments peak oxidation (Ep) of NADH at bare GC electrode occurred at +625 mV versus Ag/AgCl. Graphene oxide (GC_GO)-modified electrodes were able to detect NADH at Ep = +525 mV versus Ag/AgCl, lowering by 100 mV the potential but with a concomitant decrease (roughly 50 %) in current intensity. Graphene-modified GC electrode was able to drop further the overpotential at Ep = +280 mV versus Ag/AgCl, indicating a decrease with ∼350 mV when compared with the bare GC (Fig. 3a). Also in this case, as reported by Keeley et al. [48] and Goh and Pumera [7], the electrocatalytic effect was ascribed to the presence of large electrochemically active area of graphene [10] and edge-plane sites on multi-layered graphene, since it is no particular advantage in using monolayer graphene instead of few- or multi-layer graphene as electrode material. Ascorbic acid (AA) is one of the most common interfering specie in the electrochemical determinations of NADH. Nonetheless, ascorbic acid capitalized also on the large electrochemically active area of the graphene and its edge-plane sites, the anodic oxidation peak being situated at ∼+400 mV versus Ag/AgCl (Fig. 3b). In amperometry ascorbic acid produced a significant positive interference (+125 %, for 10^{-4} mol L^{-1} ascorbic acid and NADH). This relevant issue is acute for the majority of the carbon-based modified electrodes and could be minimized either by electrochemical pre-treatments [49] or by using ascorbate oxidase [50].

The reluctant behaviour of GO to further promote the electron transfer reaction or to improve the electrochemical properties of the GC electrode can be ascribed to its conductivity, smaller than that of graphene; moreover GO has a resistivity of about 188–413 kΩ/m [51] and, by nature, is
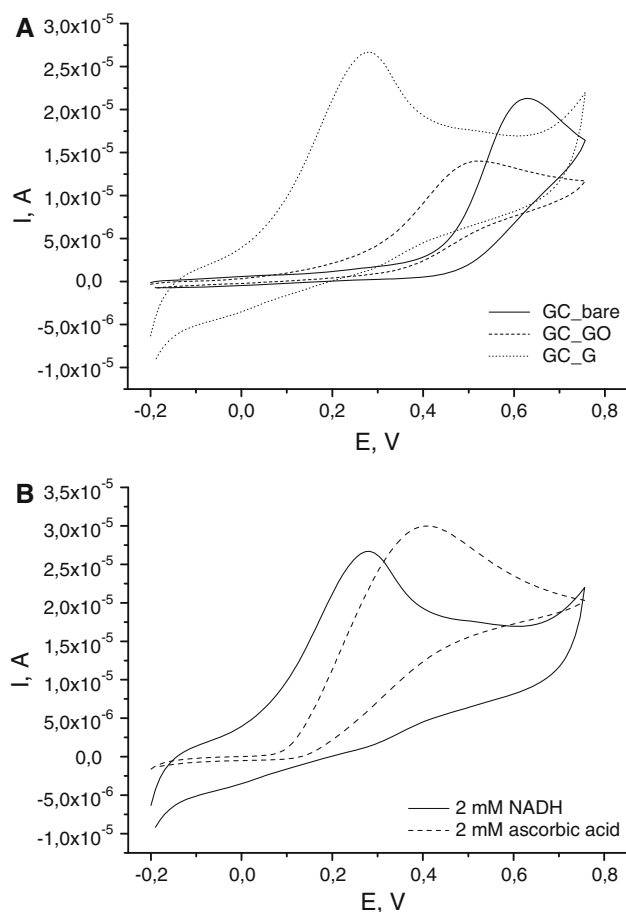

Fig. 3 Cyclic voltammetry recordings (50 mV/s) illustrating: **a** the behaviour of bare glassy carbon electrode (GC_bare), graphene (GC_G) and graphene oxide (GC_GO)-modified electrodes in the presence of 2 mM NADH, **b** the behaviour of graphene-modified electrode in the presence of NADH and ascorbic acid

considered as an insulating nanomaterial [52]. Amperometric measurements carried out at constant applied potential (+250 mV vs Ag/AgCl reference electrode), performed in a stirred solution at pH 7.4, clearly indicated that the modified electrode is suited as NADH amperometric sensor (Fig. 4). It can be observed that a nonlinear dependence of the anodic current on NADH cofactor concentration in the whole calibration range was obtained, as would be anticipated for a Michaelis-Menten type process. When considering GO-modified GC electrode, the linear working range (LWR) was very narrow, comprised between $1 \times 10^{-4} \div 2.5 \times 10^{-3}$ M (RSD = 6.5 %, $n = 3$, $y = 5.8 \times 10^{-8} + 0.1 \times 10^{-3}$ X, $r = 0.9969$), while the multi-layered graphene-modified GC electrode displayed improved analytical features (LWR = $5 \times 10^{-6} \div 1 \times 10^{-4}$ M, RSD = 4.5 %, $n = 3$, $y = 4 \times 10^{-9} + 11.1 \times 10^{-3}$ X, $r = 0.99458$). The limit of detection (LOD) was calculated as $3s_b/S$, where s_b is the standard deviation of the blank signal and S is the sensitivity. For the GO-modified GC electrode,
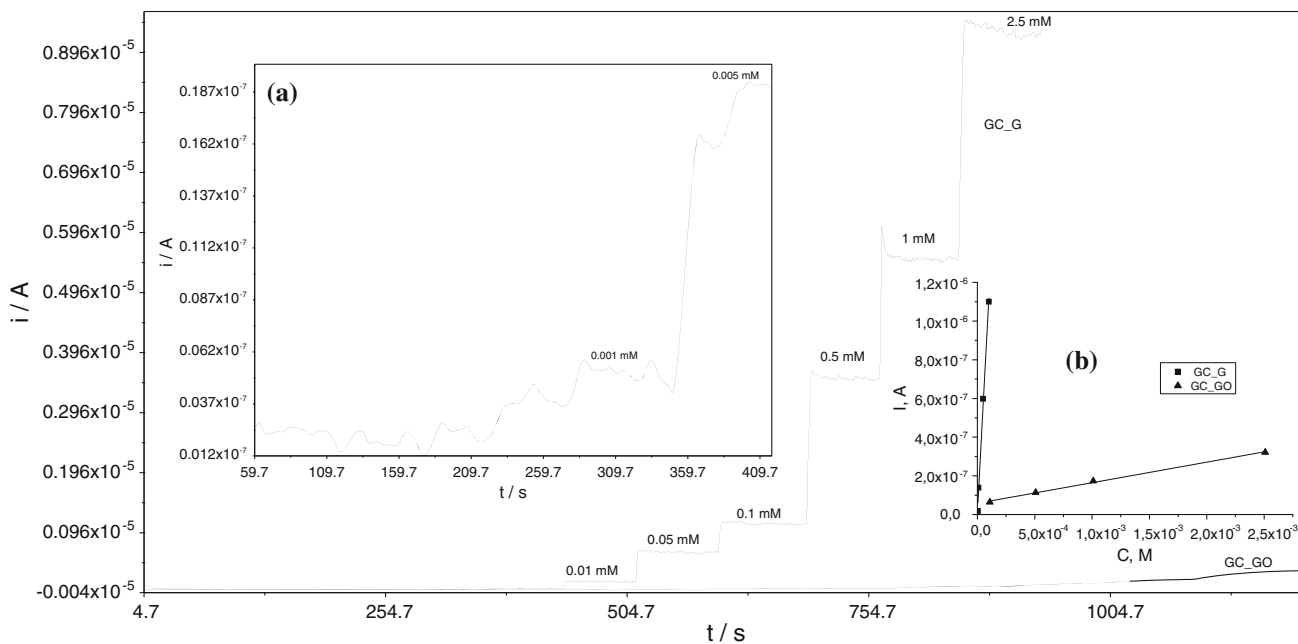
Fig. 4 Amperometric recordings of the graphene (GC_G) and graphene oxide (GC_GO)-modified electrodes in the presence of successive additions of NADH in supporting electrolyte, *inset* **a** illustrates the response of GC_G electrode in the presence of 0.001 and 0.005 mM NADH and *inset* **b** depicts the linear working ranges for GC_G and GC_GO electrodes
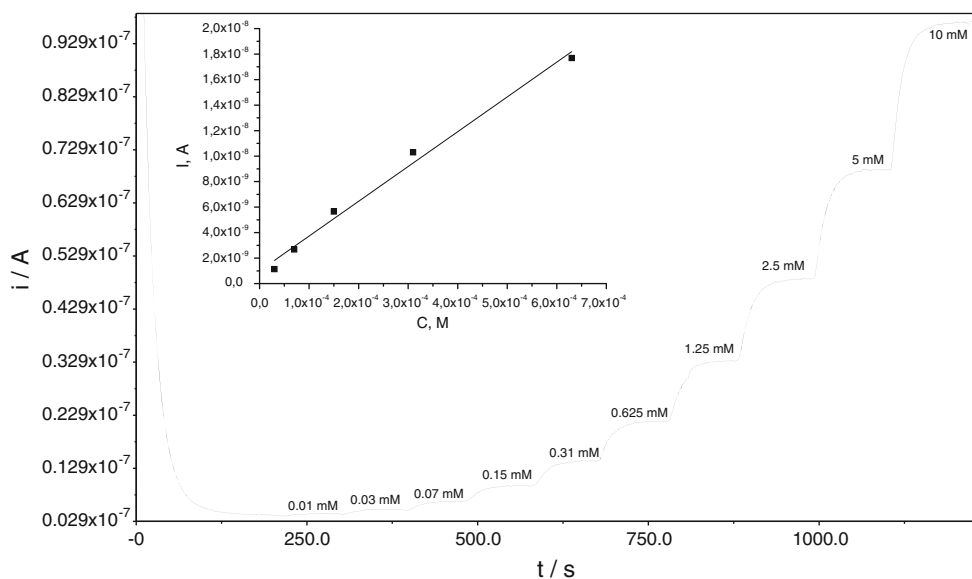

Fig. 5 Amperometric recordings of the L-Lactate biosensor in the presence of successive additions (0.5, 1.0, 2.0, 4.0, 8.0, 16, 32, 64, 128, 256 μL of 0.1 M L-lactic acid in 5 mL constant cell volume) in supporting electrolyte (10 mM phosphate buffer saline (PBS) + 0.1 M KCl, pH 7.4); *inset* the linear working range is depicted

the calculated LOD was 1×10^{-4} M, meanwhile for the graphene-modified GC electrode, the LOD was 1.0×10^{-6} M.

3.4 L-lactic acid determination in yogurts

L-lactate biosensor was developed relaying on the GC electrode modified with multi-layered graphene. L-lactic acid in the presence of the oxidised form of β-nicotinamide adenine dinucleotide (NAD$^+$) is enzymatically converted to pyruvic acid, in the presence of (L-LDH) (Equation 1).

$$\text{L-lactic acid} + \text{NAD}^+ \xrightleftharpoons{\text{L-LDH}} \text{Pyruvic acid} + \text{NADH} + \text{H}^+ \qquad (1)$$
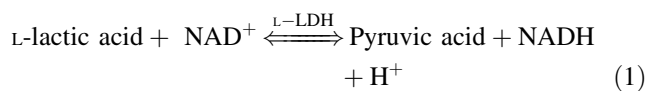
Table 1 Analytical features of several L-lactic acid biosensors reported in literature

No.	Sensing scheme	Linear working range (mM)	Limit of detection (LOD, μM)	Sensitivity (μA/mM)	E_{appl} (V)	Reference
1	Fe$_3$O$_4$/MWCNT composite	0.05–0.5	5.0	7.67	0.0 vs Ag/AgCl	[59]
2	Poly-5,2′-5′,2″-terthiophene-3′-carboxylic acid/MWNT	0.005–0.09	1.0	10.6	+0.3 vs Ag/AgCl	[12]
3	3-Mercaptopropyl-trimethoxysilane/gold nanoparticles	0–0.8	0.1	446	−0.065 vs Ag/AgCl	[60]
4	MWNT/Meldola's Blue/carbon paste	0.1–10	7.5	3.46	0.0 vs SCE	[61]
5	SWCNT/Variamine blue	0.005–0.45	1.0	–	+0.2 vs Ag/AgCl	[62]
6	Carbon hollow spheres	0.0005–0.012	3.7 ± 0.2	4.1 ± 0.2	+0.15 vs Ag/AgCl	[63]
7	Multi-layered graphene	0.03–0.6	19	–	+0.25 vs Ag/AgCl	This work

Table 2 L-lactic acid content in several yogurt types from local supermarkets

Sample	Fat (%)	Biosensor		Spectrophotometric assay
		Dilution (v/v)	Lactic acid content (%)	Lactic acid content (%)
1	0	1/200	0.33	0.35
2	2	1/200	0.48	0.45
3	3.5	1/400	0.52	0.55
4	5	1/400	0.61	0.68

Amperometric sensing of L-lactic acid in samples was achieved by coupling the L-lactate dehydrogenase with the sensor for NADH. Based on equation 2, NADH was oxidised at the electrode, thus producing an oxidation current directly proportional with the L-lactic acid concentration.

$$NADH \Rightarrow NAD^+ + H^+ + 2e^- \qquad (2)$$
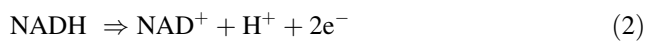
Finally, a calibration plot for L-lactic acid, in buffer, was generated (Fig. 5). The linear working range was comprised between 3×10^{-5} and 6×10^{-4} M, and the calculated LOD was 1.9×10^{-5} M (LOD was calculated as 3sb/S, where sb is the standard deviation of the blank signal and S is the sensitivity). Table 1 summarise the analytical characteristics of the developed biosensor compared to previously L-lactic biosensors reported in literature. The results obtained, using the L-lactate biosensor, were compared with the data from the colorimetric kit for L-lactic acid determination acid in foodstuffs, obtaining a good degree of correlation. The content of L-lactic acid in yogurt samples is illustrated in Table 2.

Lactose, milk fat, proteins, citrates and their enzymatic degradation products are considered as the source of flavour compounds in yogurt. During milk incubation with yogurt cultures, minimum 15 % of lactose is fermented to lactic acid, the degree of lactose utilisation and the rate of lactic acid production depending on bacteria and their symbiotic effect [53–55]. It has been reported that lactic acid sources in yogurts can be considered both proteins and fat, beside lactose [56–58]. Taking this into consideration, we consider the estimated L-lactic acid content in the analysed yogurts correlates well both with the increasing fat content (from 0 % up to 5 %) and with the data reported in literature [56–58].

4 Conclusions

Pristine graphene platelets and GO were used as electrode modifiers, aiming the investigation of their electrochemical efficacy towards NADH. The peak potential separation (ΔE) of the unmodified GC electrode in the presence of 1 mM ferricyanide was 110 mV, while after the modification of GC with graphene and GO, the electrode peak potential separation was 70 mV and 100 mV, respectively. When NADH, our analyte of interest was used, cyclic voltammetry experiments revealed that the graphene-modified GC was able to decrease the anodic peak potential with ∼350 mV, when compared with the bare GC, meanwhile in the case of GO-modified electrode the decrease was relatively moderate, i.e. ∼100 mV. Relying on the graphene-modified transducer, (L-LDH) was successfully immobilised in a 1 % Nafion® membrane. The developed biosensor, working at +250 mV versus Ag/AgCl reference electrode, was used to assess L-lactic acid in four different types of yogurts, revealing an L-lactic acid concentration ranging between 0.3 and 0.6 %. The analytical performances of the biosensor reported were more or less similar in terms of linear range and detection limits (in the micromolar range) and were comparable with those of the L-lactic acid biosensor reported in literature [59–63].

References

1. Paek E, Pak AJ, Kweon KE, Hwang GS (2013) On the origin of the enhanced supercapacitor performance of nitrogen-doped graphene. J Phys Chem C 117:5610–5616
2. Messina R, Ben-Abdallah P (2013) Graphene-based photovoltaic cells for near-field thermal energy conversion. Sci Rep 3:1383
3. Teng M-Y, Liu K-S, Cheng H-F, Lin I-N (2003) Electron field emission properties of carbon nanostructure synthesized by catalyst assisted solid-state growth process. Diam Relat Mater 12:450–455
4. Chen J, Zheng X, Miao F, Zhang J, Cui X, Zheng W (2012) Engineering graphene/carbon nanotube hybrid for direct electron transfer of glucose oxidase and glucose biosensor. J Appl Electrochem 42:875–881
5. Ajayan PM (2001) Carbon Nanotubes: Synthesis, Structure, Properties, and Applications. Springer, NewYork
6. Geim AK, Novoselov KS (2007) The rise of graphene. Nature 6:183–191
7. Goh MS, Pumera M (2010) The electrochemical response of graphene sheets is independent of the number of layers from a single graphene sheet to multilayer stacked graphene platelets. Chem Asian J 5:2355–2357
8. Du X, Skachko I, Barker A, Andrei EY (2008) Approaching ballistic transport in suspended graphene. Nature Nanotechnol 3:491–495
9. Kampouris DK, Banks CE (2010) Exploring the physicoelectrochemical properties of graphene. Chem Commun 46:8986–8988
10. Stoller MD, Park SJ, Zhu YW, An JH, Ruoff RS (2008) Graphene-based ultracapacitors. Nano Lett 8:3498–3502
11. Park S, Ruoff RS (2009) Chemical methods for the production of graphenes. Nature Nanotechnol 4:217–224
12. Rahman MM, Shiddiky MJA, MdA Rahman, Shim Y-B (2009) A lactate biosensor based on lactate dehydrogenase/nictotinamide adenine dinucleotide (oxidized form) immobilized on a conducting polymer/multiwall carbon nanotube composite film. Anal Biochem 384:159–165
13. Creanga C, El Murr N (2011) Development of new disposable NADH biosensors based on NADH oxidase. J Electroanal Chem 656:179–184
14. Meng L, Wu P, Chen G, Cai C, Sun Y, Yuan Z (2009) Low potential detection of glutamate based on the electrocatalytic oxidation of NADH at thionine/single-walled carbon nanotubes composite modified electrode. Biosens Bioelectron 24:1751–1756
15. Radoi A, Compagnone D, Batič M, Klinčar J, Gorton L, Palleschi G (2007) NADH screenprinted electrodes modified with zirconium phosphate Meldola Blue and Reinecke salt. Application to the detection of glycerol by FIA. Anal Bioanal Chem 387(3):1049–1058
16. Pereira AC, Aguiar MR, Kisner A, Macedo DV, Kubota LT (2007) Amperometric biosensor for lactate based on lactate dehydrogenase and Meldola Blue coimmobilized on multi-wall carbon-nanotube. Sensor Actuat B-Chem 124:269–276
17. Jena BK, Raj CR (2006) Electrochemical biosensor based on integrated assembly of dehydrogenase enzymes and gold nanoparticles. Anal Chem 78:6332–6339
18. Hart P, Serban S, Jones LJ, Biddle N, Pittson R, Drago GA (2006) Selective and rapid biosensor integrated into a commercial handheld instrument for the measurement of ammonium ion in sewage effluent. Anal Lett 39:1657–1667
19. Gorton L (2002) Encyclopedia of Electrochemistry. Wiley, Hoboken
20. Clark WM (1972) Oxidation–Reduction Potentials of Organic System. Krieger Publishing, Melbourne
21. Pumera M, Scipioni R, Iwai H, Ohno T, Miyahara Y, Boero M (2009) A mechanism of adsorption of b-nicotinamide adenine dinucleotide on graphene sheets: experiment and theory. Chem Eur J 15:10851–10856
22. Musameh M, Wang J, Merkoci A, Lin Y (2002) Low-potential stable NADH detection at carbon-nanotube-modified glassy carbon electrodes. Electrochem Commun 4:743–746
23. Gorton L, Domınguez E (2002) Electrocatalytic oxidation of NAD(P)H at mediator modified electrodes. Rev Mol Biotech 82:371–392
24. Gligor D, Muresan LM, Dumitru A, Popescu IC (2007) Electrochemical behavior of carbon paste electrodes modified with methylene green immobilized on two different X type zeolites. J Appl Electrochem 37:261–267
25. Délécouls-Servat K, Bergel A, Basséguy R (2001) Surface-modified electrodes for NADH oxidation in oxidoreductase-catalysed synthesis. J Appl Electrochem 31:1095–1101
26. Agui L, Yanez-Sedeno P, Pingarron JM (2008) Role of carbon nanotubes in electroanalytical chemistry: a review. Anal Chim Acta 622:11–47
27. Munteanu G, Dempsey E, McCormac T, Munteanu C (2012) Fast cyclic voltammetry of redox system NAD +/NADH on the copper nanodoped mercury monolayer carbon fiber electrode. J Electroanal Chem 665:12–19
28. Wang Y, You C, Zhang S, Kong J, Marty J-L, Zhao D, Liu B (2009) Electrocatalytic oxidation of NADH at mesoporous carbon modified electrodes. Microchim Acta 167:75–79
29. Rao TN, Yagi I, Miwa T, Tryk DA, Fujishima A (1999) Electrochemical oxidation of NADH at highly boron-doped diamond electrodes. Anal Chem 71:2506–2511
30. Radoi A, Litescu S-C, Eremia SAV, Miu M, Danila M, Dinescu A, Radu G-L (2011) Electrochemical investigation of a glassy carbon electrode modified with carbon nanotubes decorated with (poly)crystalline gold. Microchimica Acta 175:97–104
31. Xing X, Shao M, Liu CC (1996) Electrochemical oxidation of dihydronicotinadmide adenine dinucleotide (NADH) on single crystal gold electrodes. J Electroanal Chem 406:83–90
32. Aydoğdu G, Zeybek DK, Zeybek B, Pekyardımci S (2013) Electrochemical sensing of NADH on NiO nanoparticles-modified carbon paste electrode and fabrication of ethanol dehydrogenase-based biosensor. J Appl Electrochem 43:523–531
33. Shao Y, Wang J, Wu H, Liu J, Aksay IA, Lina Y (2010) Graphene based electrochemical sensors and biosensors: a review. Electroanalysis 22:1027–1036
34. Kuila T, Bose S, Khanra P, Mishra AK, Kim NH, Lee JH (2011) Recent advances in graphene-based biosensors. Biosens Bioelectron 26:4637–4648
35. Ping J, Wang Y, Fan K, Wu J, Ying Y (2011) Direct electrochemical reduction of graphene oxide on ionic liquid doped screen-printed electrode and its electrochemical biosensing application. Biosens Bioelectron 28:204–209
36. Guo K, Qian K, Zhang S, Kong J, Yu C, Liu B (2011) Bioelectrocatalysis of NADH and ethanol based on graphene sheets modified electrodes. Talanta 85:1174–1179
37. Shan C, Yang H, Han D, Zhang Q, Ivaska A, Niu L (2010) Electrochemical determination of NADH and ethanol based on ionic liquid-functionalized graphene. Biosens Bioelectron 25:1504–1508
38. Zhou M, Zhai Y, Dong S (2009) Electrochemical sensing and biosensing platform based on chemically reduced graphene oxide. Anal Chem 81:5603–5613
39. Hummers WS Jr, Offeman RE (1958) Preparation of Graphitic Oxide. J Am Chem Soc 80:1139–1339
40. Obreja AC, Cristea D, Gavrila R, Schiopu V, Dinescu A, Danila M, Comanescu F (2011) Functionalized graphene/poly 3-hexyl thiophene based nanocomposites. Proceedings of the International Semiconductor Conference 6095703:27–30

41. Stankovich S, Piner RD, Chen X, Wu N, Nguyen ST, Ruoff RS (2006) Stable aqueous dispersions of graphitic nanoplatelets via the reduction of exfoliated graphite oxide in the presence of poly(sodium 4-styrenesulfonate). J Mater Chem 16:155–158

42. Dikin DA, Stankovich S, Zimney EJ, Piner RD, Dommett GHB, Evmenenko G, Nguyen SBT, Ruoff RS (2007) Preparation and characterization of graphene oxide paper. Nature 448:457–460

43. Brownson DAC, Munro LJ, Kampouris DK, Banks CE (2011) Electrochemistry of graphene: not such a beneficial electrode material? RSC Adv. 1:978–988

44. Brownson DAC, Kampouris DK, Banks CE (2012) Graphene electrochemistry: fundamental concepts through to prominent applications. Chem Soc Rev 41:6944–6976

45. Goh MS, Pumera M (2010) Single-, few- and multilayer graphene do not exhibit significant advantages over graphite microparticles in electroanalysis. Anal Chem 82:8367–8370

46. Li W, Tan C, Lowe MA, Abruna HD, Ralph DC (2011) Electrochemistry of individual monolayer graphene sheets. ACS Nano 5:2264–2270

47. Valota AT, Kinloch IA, Novoselov KS, Casiraghi C, Eckmann A, Hill EW, Dryfe RAW (2011) Electrochemical behavior of monolayer and bilayer graphene. ACS Nano 5:8809–8815

48. Keeley GP, O'NeillA Holzinger M, Cosnier S, Coleman JN, Duesberg GS (2011) DMF-exfoliated graphene for electrochemical NADH detection. Phys Chem Chem Phys 13:7747–7750

49. Deng C, Peng Y, Su L, Liu Y-N, Zhou F (2012) On-line removal of redox-active interferents by a porous electrode before amperometric blood glucose determination. Anal Chim Acta 719:52–56

50. Matsumoto K, Tsukatani T, Okajima Y (1995) Amperometric flow-injection determination of citric acid in food using free citrate lyase and coimmobilized oxalacetate decarboxylase and pyruvate oxidase. Electroanalysis 7:527–530

51. Su CY, Xu Y, Zhang W, Zhao J, Liu A, Tang X, Tsai CH, Huang Y, Li LJ (2010) Highly efficient restoration of graphitic structure in graphene oxide using alcohol vapors. ACS Nano 4:5285–5292

52. Stankovich S, Dikin DA, Piner RD, Kohlhaas KA, Kleinhammes A, Jia Y, Wu Y, Nguyen SBT, Ruoff RS (2007) Synthesis of graphene-based nanosheets via chemical reduction of exfoliated graphite oxide. Carbon 45:1558–1565

53. Baranowska M (2006) Intensification of the synthesis of flavour compounds in yogurt by milk enrichment with their precursors. Pol J Food Nutr Sci 56:5–11

54. Rasic JL, Kurmann JA (1978) Yoghurt. Scientific Grounds, Technology, Manufacture and Preparations. Technical Dairy Publishing House, Copenhagen

55. Lourens-Hattingh A, Viljoen BC (2001) Yogurt as probiotic carrier food. Int Dairy J 11:1–17

56. Nakazawa Y, Hasono A (1992) Functions of Fermented Milk Challenges for the Health Science. Elsevier Applied Science Publisher, Amsterdam

57. Nakazawa Y, Hasono A (1992) Functions of Fermented Milk. Elsevier Applied Science, Amsterdam

58. Khusniati T, Ardina A, Choliq A (2011) Lactic acid content and b-galactosidase activity of yoghurt with starter added Bifidobacteria bifidum at storage and its organoleptic test. Berk Penel Hayati 4C:79–82

59. Teymourian H, Salimi A, Hallaj R (2012) Low potential detection of NADH based on Fe_3O_4 nanoparticles/multiwalled carbon nanotubes composite: fabrication of integrated dehydrogenase-based lactate biosensor. Biosens Bioelectron 33:60–68

60. Jena BK, Raj CR (2007) Amperometric L-lactate biosensor based on gold nanoparticles. Electroanalysis 7–8:816–822

61. Pereira AC, Aguiar MR, Kisner A, Macedo DV, Kubota LT (2007) Amperometric biosensor for lactate based on lactate dehydrogenase and Meldola Blue coimmobilized on multi-wall carbon-nanotube. Sens Act B 124:269–276

62. Radoi A, Compagnone D, Valcarcel MA, Placidi P, Materazzi S, Moscone D, Palleschi G (2008) Detection of NADH via electrocatalytic oxidation at single-walled carbon nanotubes modified with Variamine blue. Electrochimica Acta 53:2161–2169

63. Gao F, Guo X, Yin J, Zhao D, Li M, Wang L (2011) Electrocatalytic activity of carbon spheres towards NADH oxidation at low overpotential and its applications in biosensors and biofuel cells. RSC Adv 1:1301–1309